



LUND UNIVERSITY

Comparing Analog Front-Ends for Duty-Cycled Wake-Up Receivers in Wireless Sensor Networks

Seyed Mazloun, Nafiseh; Edfors, Ove

Published in:
IEEE Sensors Journal

DOI:
[10.1109/JSEN.2016.2593059](https://doi.org/10.1109/JSEN.2016.2593059)

2016

Document Version:
Other version

[Link to publication](#)

Citation for published version (APA):
Seyed Mazloun, N., & Edfors, O. (2016). Comparing Analog Front-Ends for Duty-Cycled Wake-Up Receivers in Wireless Sensor Networks. *IEEE Sensors Journal*, 16(18), 7016 - 7021.
<https://doi.org/10.1109/JSEN.2016.2593059>

Total number of authors:
2

General rights

Unless other specific re-use rights are stated the following general rights apply:
Copyright and moral rights for the publications made accessible in the public portal are retained by the authors and/or other copyright owners and it is a condition of accessing publications that users recognise and abide by the legal requirements associated with these rights.

- Users may download and print one copy of any publication from the public portal for the purpose of private study or research.
- You may not further distribute the material or use it for any profit-making activity or commercial gain
- You may freely distribute the URL identifying the publication in the public portal

Read more about Creative commons licenses: <https://creativecommons.org/licenses/>

Take down policy

If you believe that this document breaches copyright please contact us providing details, and we will remove access to the work immediately and investigate your claim.

LUND UNIVERSITY

PO Box 117
221 00 Lund
+46 46-222 00 00

Comparing Analog Front-ends for Duty-cycled Wake-up Receivers in Wireless Sensor Networks

Nafiseh Seyed Mazloun and Ove Edfors

Department of Electrical and Inform. Technology, Lund University, Lund, Sweden

Email: {nafiseh.seyed_mazloun, ove.edfors}@eit.lth.se

Abstract—Using ultra low-power wake-up receivers (WRxs) can reduce idle listening energy cost in wireless sensor networks with low traffic intensity. This has led to many WRx analog front-end (AFE) designs presented in literature, with a large variety of trade-offs between sensitivity, data rate, and power consumption. Energy consumed during wake-up in a network depends on many parameters and without a unified energy analysis, we cannot compare performance of different AFEs. We present an analysis of duty-cycled WRx schemes which provides a simple tool for such a comparison, based on the energy consumed in an entire single-hop network during a wake-up. The simplicity is largely due to the fact that all network and communication parameter settings can be condensed into a single scenario constant. This tool allows us to both compare AFEs for specific scenarios and draw more general conclusions about AFE performance across all scenarios.

Index Terms—Wake-up receiver, low-power, front-end, duty-cycle, performance comparison.

I. INTRODUCTION

The use of an extra ultra-low power receiver, typically referred to as a wake-up receiver (WRx), is accounted as a practical solution to reduce idle channel monitoring energy cost in wireless sensor network applications with low traffic intensity [1]. This is particularly important in networks with limited energy resources. An ultra-low power WRx monitors the wireless channel while the nodes high power main receiver is switched off. The WRx powers up the main receiver only when a wake-up beacon (WB) is detected. There are two main approaches for how a WRx monitors the channel. A WRx can be always on [1], [2] or it can be duty-cycled [3], [4]. While the always-on approach allows for short wake-up delays, the system average power consumption is relatively high as it cannot go below the (always-on) WRx power consumption. The duty-cycling approach, on the other hand, is more energy efficient as WRxs sleep most of the time. The associated drawback is, of course, longer wake-up delays. By introducing a requirement on average delay [4] we can, however, optimize sleep intervals to also meet requirements for delay sensitive applications. With this work we assume that nodes operate according to duty-cycled WRx scheme principles and compare WRx analog front-end (AFE) performances for this type of WRx schemes.

To save power a WRx needs to operate at a very limited power consumption, typically two orders of magnitude lower than the main receiver, e.g., in the order of $10\mu\text{W}$ [1], [5]. A large fraction of total power is consumed in the AFE of a WRx and many front-end architectures have been proposed to meet

strict low-power requirements [6]–[27]¹. Simple non-coherent modulation schemes, e.g., on-off keying (OOK) [6]–[12], [14], [15], [19]–[24], [27], binary frequency shift-keying (BFSK) [16]–[18], pulse position modulation (PPM) [25], and pulse width modulation (PWM) [13], [26], are often chosen for WB transmission, since they allow low-power low-complex AFE designs. In literature WRx AFEs are typically evaluated by their sensitivity, related to a BER of 10^{-3} , and their corresponding power consumption. Both these at some operating frequency and data rate suitable for the scenario at hand. The ones listed above are no exception to this. In [21] a figure-of-merit also based on sensitivity, power consumption, and data rate, is introduced. While these measures are important for the individual AFE designs, they are not sufficient if we want to compare how WRx AFEs influence total wake-up energy consumption in a network. Extreme low-power design of an AFE typically leads to a high noise figure and degraded sensitivity, compared to the main receiver. High WB transmit power required to compensate for the reduced sensitivity can lead to an energy cost substantially higher than the energy saving obtained from using a low-power WRx. Therefore, a comparison needs to include both transmit and receive energy costs. By calculating the total energy required in a network to perform a wake-up, we enable such a comparison. Our measure takes both channel listening and WB transmission costs into account and makes WRx AFE design comparisons dependent on scenario parameters like network size, coverage needed, and limitations on average wake-up delays.

In Section II, we describe the overall operation of a duty-cycled WRx scheme. A simple expression is developed for the energy analysis of the addressed system in Section III. By studying the energy model in Section IV we obtain insight into how changes in WRx AFE characteristics and system parameters relate to energy consumption attributed to wake-ups. Using this simple energy model we illustrate how to compare the wake-up energy performance of WRx AFEs for different network settings and channel conditions and single out the best performing ones. Conclusions and final remarks are presented in Section V.

II. SYSTEM OVERVIEW

In our reference system all nodes are equal and communicate in a single-hop fashion according to the addressed duty-

¹WRxs are proposed for different data communication channels such as radio frequency (RF), infrared, ultrasound, and body coupled communication (for WBAN). This study includes only RF based WRx designs.

cycled WRx scheme. With all nodes in the network being equal, limitation of energy costs for WB transmission and reception are of equal importance. Each node consists of a transmitter, a main receiver, and a duty-cycled WRx. The principle of communication in a single-hop network of N nodes with packet inter-arrival interval $1/\lambda$ is as follows. The WRxs of all nodes listen periodically and asynchronously to the channel for a WB. Both the transmitter and the main receiver are switched off. A node with data available for transmission, called the source node, turns on its transmitter and initiates communication by transmitting strobed WBs ahead of the data. These WBs carry both source and destination node addresses to avoid overhearing by non-destination nodes [28]. When a WB transmission coincides with the WRx listen interval of the destination node, the WRx detects the WB and turns on the transmitter to reply with a wake-up acknowledgment (WACK). It also prepares for data reception by turning on the main receiver.

Ideally no error occurs when detecting a WB, but in a real system there exist both noise and interference. Therefore, there is a certain probability that the transmitted WB is missed by the WRx or the WRx erroneously detects a WB. The latter can occur both when only noise/external interference is received or, when a WB addressed to another node is present on the channel. Subsequently, not only does the chosen duty cycle of the WRx determine the energy cost of channel listening, together with WB error probabilities it also influences transmission cost through the number of WBs that needs to be transmitted to perform a wake-up. Through these mechanisms WRx characteristics, in terms of sensitivity and power consumption, have direct impact on transmit and receive energy consumption and thereby on total wake-up energy cost.

III. WAKE-UP ENERGY ANALYSIS

With a direct relation, as discussed above, between WRx characteristics and total energy required for a wake-up, we calculate this energy and use it as basis for comparing WRx AFE designs. With limited battery resources, we can see it as a ranking of WRx AFEs according to resulting battery life times. The comparison relies on everything but AFEs being equal.

Independent of the WRx front-end used, the WB length (counted in bits) has to be the same to achieve the same WB detection performance when operating at the same channel BER. This can be used to simplify our calculations by focusing on the energy required to receive one bit in the WB waking up our receiver. We also assume that node power consumption in sleep mode is insignificant compared to that in other modes. The rationale behind this is found in, e.g., [29] where sleep power consumption is between five and seven orders of magnitude lower than the WRx and transmitter/main receiver power consumptions. WB detection performance, in terms of WB miss and false-alarm probabilities, has been extensively studied in [30] for a WB consisting of a preamble and an address part. The preamble is used to provide synchronization and the address part is necessary to avoid overhearing. Additionally, to limit WB miss and false alarm error probabilities,

we select the preamble from sequences with good auto-correlation properties and apply spreading on the address bits. This also provides protection against external interference. WB parameters have been optimized for a wide range of channel BERs in [30], but WRx front-end sensitivity figures in literature are often measured at 10^{-3} BER, making it an attractive reference point² in the analysis. This low BER also results in very rare WB detection errors, making it possible to ignore their influence on energy consumption and thereby further simplify the analysis.

Given the above, total wake-up energy per data packet is calculated as the sum of periodic WB transmissions by the source node and duty-cycled channel listening, by all N nodes, during an average packet arrival interval. Calculated per received WB bit, it becomes

$$E_{tot} = W P^{tx} T_b + K N P^{wrx} T_b, \quad (1)$$

where W is the average number of WB transmissions needed for a wake-up, P^{tx} the transmitter power consumption, T_b the bit time, K the number of WRx duty-cycles per average packet-arrival interval, and P^{wrx} the WRx power consumption.

We can calculate W in (1) as half the number of WBs that fit in one WRx duty cycle of length $(1/\lambda)/K$, since nodes are asynchronous and no data packet arrival time is more likely than any other. With Z_{wb} bits in a WB, each has a length of $Z_{wb} T_b$ and we get

$$W = \frac{1/\lambda}{2K Z_{wb} T_b}. \quad (2)$$

As expected, K and W are inversely related. The more frequently the WRx duty cycles, the fewer WBs need to be transmitted before a wake-up. By changing K we can control the resulting average wake-up delay. To meet an average wake-up delay requirement of D^{req} , we set

$$K = \frac{1/\lambda}{2D^{req}}. \quad (3)$$

Next we relate transmitter power consumption P^{tx} in (1) to WRx AFE sensitivity P_s^{wrx} through the largest expected propagation loss $L_{p,max}$ and transmitter efficiency η as³

$$P^{tx} = \frac{P_s^{wrx} L_{p,max}}{\eta}, \quad (4)$$

where η refers to the ratio of actual transmitted power and transmitter power consumption. Substituting (2), (3), and (4) back in (1), and defining the WRx energy consumption per bit

$$E^{wrx} = P^{wrx} T_b, \quad (5)$$

we get

$$E_{tot} = \frac{D^{req} L_{p,max}}{\eta Z_{wb}} P_s^{wrx} + N \frac{1/\lambda}{2D^{req}} E^{wrx}, \quad (6)$$

²Since WRxs AFEs typically have the same type of exponential BER characteristic, a change of BER reference point or any applied coding changes the WRxs absolute energy levels but has no effect on their relative ranking, as long as we can assume rare WB detection errors.

³Propagation loss $L_{p,max}$ is a number larger than one and transmitter efficiency η is a number smaller than one.

showing that wake-up energy consumption depends on more parameters than AFE sensitivity and energy consumption per bit. The additional parameters, constituting the scenario, are delay requirement, maximum propagation loss, transmitter efficiency, WB length, network size, and traffic. An important feature of (6) is that it does not depend on data rate, or bandwidth, making it possible to compare WRx designs with quite different design specifications when operated in the same scenario.

IV. WAKE-UP RECEIVER FRONT-END COMPARISONS

In this section we show how to use (6) to compare and evaluate energy performance of WRx AFEs. Let us first study the overall behavior of (6) for two example scenarios. Comparing front-ends across vastly different bands is not favorable as their propagation loss will be different. We therefore compare AFEs designed for the same frequency band. Our scenarios are:

Scenario 1: 2.4 GHz wireless body area network (WBAN) applications with a worst case path loss of 88 dB⁴ corresponding to ear-to-ear communication [29], [31]. We assume a network size N of 64 nodes, packet inter-arrival interval $1/\lambda$ of 1000 sec., and a 10 msec. average delay requirement D^{req} .
Scenario 2: 900 MHz short range wireless communication applications with a worst case path loss set to 55 dB [32]. For this scenario, we assume a larger network size N of 512 nodes, a lower traffic with packet inter-arrival interval $1/\lambda$ of 100000 sec., and an average delay requirement D^{req} of 0.25 second.

We set the WB length Z_{wb} to 21 and 25 bits in Scenario 1 and Scenario 2, respectively, based on optimization results in [30]. In both scenarios, we assume transmitter efficiency η of 50%. Replacing the values specified above in (6) we calculate the total energy consumption for wake-up per received WB bit. Results are shown as level curves in Fig. 1(a) with axes AFE sensitivity P_s^{wrx} and corresponding AFE energy consumption per bit E^{wrx} in dB scale⁵. Almost straight level curves stemming either from P_s^{wrx} or from E^{wrx} show that total energy consumption in most cases is dominated either by WB transmission or AFE channel listening. To illustrate for which values on P_s^{wrx} and E^{wrx} the two energy costs are balanced, we calculate what we call *balance lines* by making the two terms in (6) equal. This gives

$$P_s^{wrx} = E^{wrx} + \Gamma \text{ [dB]}, \quad (7)$$

where all scenario parameters have been condensed into a single scenario constant

$$\Gamma = N + \eta + Z_{wb} + (1/\lambda) - 2D^{req} - 3 - L_{p,max} \text{ [dB]}. \quad (8)$$

Using (7) and (8), replacing scenario parameters with values specified above, we calculate balance lines for the two scenarios, shown as diagonal lines in Fig. 1(a). Studying E_{tot}

level curves, together with their corresponding balance lines, we make several observations regarding energy consumption characteristics:

- All level curves have the same shape, are symmetric around the balance line, and shifted along it with changes in energy level.
- The total energy, as indicated in the figure, increases with increasing P_s^{wrx} and E^{wrx} .
- Changes in scenario parameters will change Γ and accordingly shift both the balance line and the corresponding level curves.

These characteristics can be used as a tool for comparing the relative merits of different WRx AFE designs, without going through complete energy calculation for the individual designs. In the following we first compare AFE performances for systems with certain parameter settings, and then provide a mechanism through which we find the set of best-performing WRx AFEs across all scenarios.

TABLE I
WAKE-UP RECEIVER (WRX) DESIGNS.

Reference ⁶	Sensitivity ⁷ [dBm]	Power cons. [μW]	Data rate [kbps]	E^{wrx} [dB(J/b)]
Pletcher ('07) [6]	-50*	65	40	-87.9
Pletcher ('09) [7]	-72*	52	100	-92.8
Durante ('09) [8]	-57*	7.5	100	-101.2
Lont ('09) [33]	-65	126	50	-86
Drago ('10) [25]	-87/-82*	415	250/500	-87.8/-90.8
Le ('10) [26]	-53*	19	50	-94
Hambeck ('11) [27]	-71	2.4	100	-106
Cheng ('12) [9]	-65*	10	100	-100
Bae ('12) [17]	-62	45	312	-98.4
Nilsson ('13) [11]	-47*	2.3	200	-109
Oh ('13) [12]	-45 -43*	0.116	12.5	-110.3
Takahagi ('13) [13]	-47.2*	6.8	500	-108.6
Milosiu ('13) [22]	-83	7.2	64	-99.5
Abe ('14) [18]	-87	45.5	50	-90.4
Bryant ('14) [20]	-88*	50	250	-97
Huang ('14) [21]	-86.5 -86 -79.5 -68.5 -61	146 123 101 84 64	10	-78.3 -79.1 -80 -80.7 -81.9
Salazar ('15) [19]	-97/-92*	99	10/50	-80/-87

A. Best performance in a specific scenario

In Fig. 1(b) we show characteristics of the AFEs listed in Table I. We replace E^{wrx} in (6) by the front-end energy consumption per bit, assuming that energy consumption of the WRx digital base-band is negligible [34], compared to that of the AFE. We are interested to find a WRx AFE among the existing solutions that is the best in terms of wake-up energy

⁴Variables are defined in linear scale, but we often assume dB scale in the text – which one should be clear from the context.

⁵Presenting P_s^{wrx} and E^{wrx} in non-dB, the level curves are straight lines, but large dynamic ranges in P_s^{wrx} and E^{wrx} make a dB scale more convenient.

⁶The sensitivity and power consumption in [12], [18] and [27] are reported for the entire WRx design. We have excluded their processing gains from sensitivity and their correlator power consumptions from the total power consumption in Fig.1(a) and Fig.3(a).

⁷Sensitivities marked by '*' are for 2.4 GHz operating frequency, all others for 780 – 950 MHz.

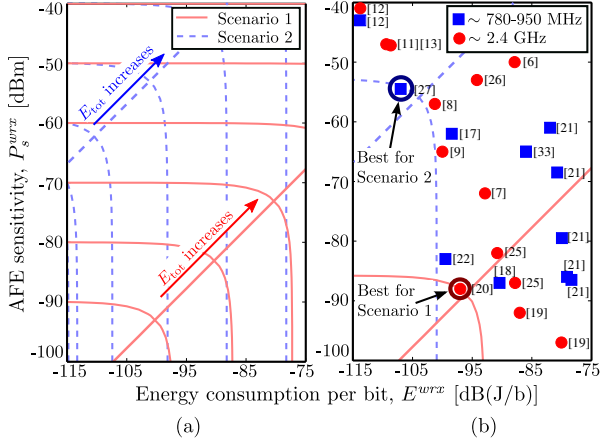


Fig. 1. (a) Total energy consumption per wake-up level curves as functions of wake-up receiver (WRx) sensitivity and energy consumption per bit for two examples scenarios. (b) Performance comparison of WRx analog front-ends listed in Table I.

performance in a certain scenario. Graphically, this can be done in two steps.

Step 1: Calculate the scenario constant Γ , using (8), for the given scenario parameters and plot the corresponding balance line (7).

Step 2: Slide a level curve, with the same shape as in Fig. 1(a), along the balance line, starting from the lower left corner, until it hits the first AFE design. This AFE provides the lowest wake-up energy consumption for that particular scenario.

Let us illustrate the above for our two example scenarios, finding the respective best-performing WRx AFEs among those listed in Table I. First we add the balance line that corresponds to each scenario (red solid and blue dashed), to Fig. 1(b). For Scenario 1, we search among the WRx AFEs designed to operate at 2.4 GHz (red dots), while for Scenario 2, we search among the ones operating at 780 – 950 MHz (blue squares). As indicated in the figure, the lowest energy consumption is obtained for the WRx AFE designs in [20] and [27] for Scenario 1 and Scenario 2, respectively.

B. Best-performing front-ends across all scenarios

Characteristics of energy level curves and balance lines can also be used to find the set of AFE designs that, for at least some scenario constant Γ , results in the lowest energy consumption compared to the other designs. Having access to such a set provides a quick and simple evaluation approach when adding/designing a new WRx AFE as we only need to compare to a smaller set of designs.

We find WRx AFEs with such characteristics by varying Γ throughout its entire range, $(-\infty, \infty)$ dB, finding the best performing AFE design for each Γ . Let us illustrate this graphically, using the two-step approach in the previous section for a large number of Γ s. First, we study only one WRx front-end design, as in Fig. 2(a). This single AFE will, trivially, be the best-performing one for all scenarios. The main point of the illustration is that the collection of level curves (gray) going through the reference AFE location create four regions,

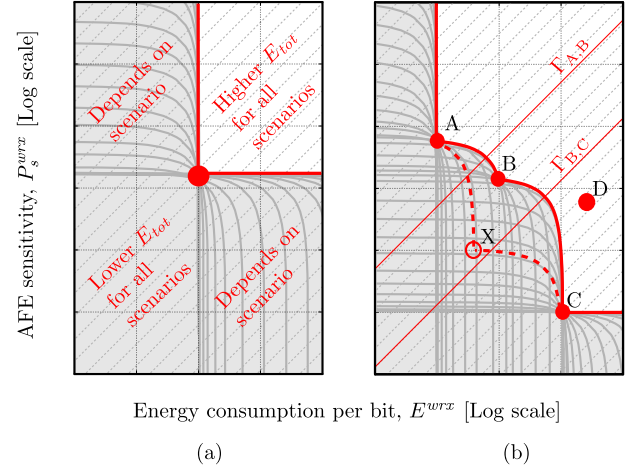


Fig. 2. Graphical illustration of finding best performing WRx AFE designs across scenarios. The trivial single-AFE case (a) and multiple AFEs (b).

or quadrants, around it. With total energy consumption E_{tot} increasing when P_s^{wrx} and E^{wrx} increase, any AFE design in the lower left quadrant always have a lower E_{tot} than the reference AFE. Correspondingly, all AFE designs in the upper right quadrant always have a higher E_{tot} than the reference AFE. The energy performance of AFE designs ending up in the other two quadrants, however, can be both better or worse in terms of energy performance, depending on scenario.

When we have more than one WRx AFE to compare we apply the same principle, sweeping over scenario constants Γ to find the best performing AFE for each scenario. The result of a simplified case with four AFEs is shown in Fig. 2(b), where AFE A is the best performing one for $\Gamma > \Gamma_{A,B}$, AFE B for $\Gamma_{A,B} > \Gamma > \Gamma_{B,C}$, and AFE C for $\Gamma < \Gamma_{B,C}$. At the boundary scenarios $\Gamma = \Gamma_{A,B}$ and $\Gamma = \Gamma_{B,C}$, two AFEs have equal energy performance – A and B in the first case and B and C in the second case. AFE D is not best performing in any scenario. A new AFE in the gray region will be added to the set of best-performing AFEs. This may also imply that other AFEs are removed from the set, as indicated in Fig. 2(b) where the new hypothetical design AFE X replaces AFE B. This changes the corresponding scenario constants (Γ s at boundary scenarios) for which AFE A, AFE X, and AFE C perform the best⁸. As we show in the following, knowing the AFEs sensitivity and energy consumption per bit we can calculate Γ s for boundary scenarios. While we explicitly perform the calculation for AFE A and AFE B in Fig. 2(b), the same calculation can be applied to any pair of AFE designs. Let $P_{s,A}^{wrx}$, $P_{s,B}^{wrx}$, E_A^{wrx} , and E_B^{wrx} be the sensitivities and energy consumptions per bit for AFEs A and B, respectively. Substituting these in (6) and setting the two obtained energy levels equal we identify the resulting boundary scenario constant

$$\Gamma_{A,B} = -\frac{P_{s,A}^{wrx} - P_{s,B}^{wrx}}{E_A^{wrx} - E_B^{wrx}}. \quad (9)$$

This uniquely defines the scenario constant for which AFEs A and B perform equally in terms of total wake-up energy.

⁸The new boundary Γ s are not shown to avoid overcrowding the figure.

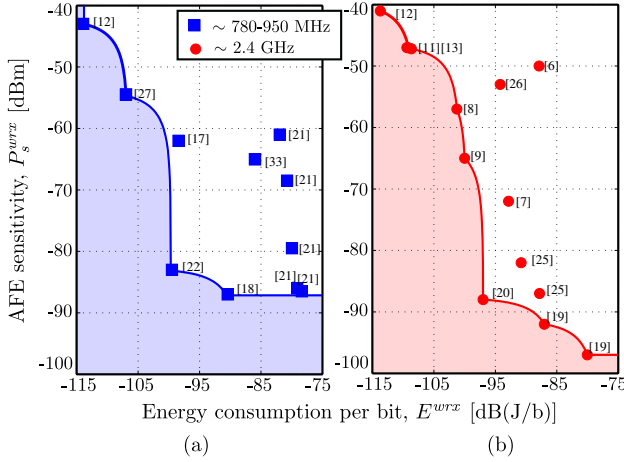


Fig. 3. Best-performing analog front-ends for WRxs operating at (a) 780 – 950 MHz and (b) 2.4 GHz.

Since the scenario constant, per definition, is a non-negative real number the ratio $(P_{s,A}^{wrx} - P_{s,B}^{wrx}) / (E_A^{wrx} - E_B^{wrx})$ has to be negative. This shows that two AFEs cannot have equal performance in any scenario if one is better both in terms of sensitivity and energy consumption per bit. It also explains the lower-left and upper-right quadrants in Fig. 2(a).

We now apply the above mechanism separately to the two WRx categories in Table I, operating at 780 – 950 MHz and 2.4 GHz. The results are shown in Fig. 3. In both sub-figures, all WRx AFE designs on the solid curve belong to the set of best performing AFEs. In the white area we see AFE designs that are not best-performing in any scenario⁹. To rank the best-performing AFEs against each other we measure the range of scenarios for which each AFE is the best-performing one. For AFE B in Fig. 2(b), this range is between boundary scenarios $\Gamma_{A,B}$ and $\Gamma_{B,C}$. By merit of being the best-performing AFE for more scenarios, a larger range is considered better. Using (9) we calculate the boundary scenario constants for all AFEs in the two sets of best performing ones AFEs shown in Fig. 3. The obtained ranges are listed in Table II. The calculation is, however, not applicable to the two designs having either the best sensitivity or the lowest energy consumption per bit. They are best for extreme scenarios, where scenario constants are either very low or very high. Among AFEs operating at 780–950 MHz [27] has the best range and among those at 2.4 GHz [20].

V. CONCLUSIONS AND REMARKS

This paper presents a system-level analysis of low-power WRx which can be used to evaluate and compare WRx AFEs with different design characteristics. We calculate the wake-up energy consumption for an entire network where nodes only wake up periodically using a duty-cycled WRx. The closed form energy expressions give us a good understanding how energy consumption is related to WRx front-end design characteristics and scenario parameters. By studying energy

⁹It should be noted that we only compare total wake-up energy consumption. AFE designs not being among the best-performing ones in this measure may have other merits that do not come through in this analysis.

TABLE II
SCENARIO CONSTANT RANGE FOR AFEs BELONGING TO THE SET OF BEST-PERFORMING AFE, (A) FOR 780–950 MHz OPERATING FREQUENCY, (B) FOR 2.4 GHz OPERATING FREQUENCY.

(a)		(b)	
Reference	Range of scenario constant (dB)	Reference	Range of scenario constant (dB)
Oh ('13) [12]	N.A. (lowest E^{wrx})	Oh ('13) [12]	N.A. (lowest E^{wrx})
Hambeck ('11) [27]	33.6	Nilsson ('13) [11]	11
Milosiu ('13) [22]	23.5	Takahagi ('13) [13]	4.3
Abe ('14) [18]	N.A. (lowest P_s^{wrx})	Durante ('09) [8]	6
		Cheng ('12) [9]	13.4
		Bryant ('14) [20]	37.7
		Salazar ('15) [19]	10
		Salazar ('15) [19]	N.A. (lowest P_s^{wrx})

consumption level curves, we propose a simple and intuitive tool for comparing existing WRx AFE designs found in literature. The tool allows us to find the best-performing AFE design for a specific scenario and draw conclusions about overall best-performing AFEs. For any given set of AFE designs, the latter analysis provides a simple mean to decide whether a new design will be among the best-performing ones or not. This is particularly valuable when setting design targets for new WRx AFE designs, if low total wake-up energy consumption in a network is the objective.

REFERENCES

- [1] C. Guo, L. C. Zhong, and J. Rabaey, "Low power distributed MAC for ad hoc sensor radio networks," in *IEEE Global Telecommun. Conf.*, 2002, pp. 2944–2948.
- [2] Y. Zhang *et al.*, "A 3.72 μ W ultra-low power digital baseband for wake-up radios," in *Int. Symp. VLSI Design, Automation and Test*, April 2011, pp. 1–4.
- [3] E.-Y. Lin, "A comprehensive study of power-efficient rendezvous schemes for wireless sensor networks," Ph.D. dissertation, University of California, Berkeley, 2005.
- [4] N. S. Mazloun and O. Edfors, "DCW-MAC: An energy efficient medium access scheme using duty-cycled low-power wake-up receivers," in *IEEE Vehicular Technol. Conf.*, September 2011, pp. 1–5.
- [5] E.-Y. Lin, J. Rabaey, and A. Wolisz, "Power-efficient rendez-vous schemes for dense wireless sensor networks," in *IEEE Int. Conf. Commun.*, vol. 7, June 2004, pp. 3769–3776.
- [6] N. Pletcher, S. Gambini, and J. Rabaey, "A 65 μ W, 1.9GHz RF to digital baseband wakeup receiver for wireless sensor nodes," in *IEEE Custom Integrated Circuits Conf.*, 2007.
- [7] N. M. Pletcher, S. Gambini, and J. Rabaey, "A 52 μ W wake-up receiver with -72dBm sensitivity using an uncertain-IF architecture," *IEEE J. Solid-State Circuits*, vol. 44, pp. 269–280, January 2009.
- [8] M. S. Durante and S. Mahlknecht, "An ultra low power wakeup receiver for wireless sensor nodes," in *Proc. 3rd Int. Conf. Sensor Technol. and Applicat.*, June 2009, pp. 167–170.
- [9] K.-W. Cheng, X. Liu, and M. Je, "A 2.4/5.8GHz 10 μ W wake-up receiver with -65/-50dBm sensitivity using direct active RF detection," *IEEE Asian Solid-State Circuits Conf.*, pp. 337–340, 2012.
- [10] J. Choi, K. Lee, S.-O. Yun, S.-G. Lee, and J. Ko, "An interference-aware 5.8GHz wake-up radio for ETCS," in *IEEE Int. Solid-State Circuits Conf. Dig. of Tech. Papers*, 2012, pp. 446–448.
- [11] E. Nilsson and C. Svensson, "Ultra low power wake-up radio using envelope detector and transmission line voltage transformer," *IEEE J. on Emerging and Select. Topics in Circuits and Syst.*, vol. 3, no. 1, pp. 5–12, 2013.
- [12] S. Oh, N. E. Roberts, and D. D. Wentzloff, "A 116nW multi-band wake-up receiver with 31-bit correlator and interference rejection," in *IEEE Custom Integrated Circuits Conf.*, 2013, pp. 1–4.
- [13] K. Takahagi, H. Matsushita, T. Iida, M. Ikebe, Y. Amemiya, and E. Sano, "Low-power wake-up receiver with subthreshold CMOS circuits for wireless sensor networks," *Analog Integrated Circuits and Signal Process.*, vol. 75, no. 2, pp. 199–205, 2013.

- [14] T. Wada, M. Ikebe, and E. Sano, "60GHz, 9 μ W wake-up receiver for short-range wireless communications," in *Proc. of the Eur. Solid State Circuits Conf.*, 2013, pp. 383–386.
- [15] J. Lee, I. Lee, J. Park, J. Moon, S. Kim, and J. Lee, "A sub-GHz low-power wireless sensor node with remote power-up receiver," in *IEEE Radio Frequency Integrated Circuits Symp.*, 2013, pp. 79–82.
- [16] M. Lont, D. Milosevic, A. van Roermund, and G. Dolmans, "Ultra-low power FSK wake-up receiver front-end for body area networks," in *IEEE Radio Frequency Integrated Circuits Symp.*, 2011, pp. 1–4.
- [17] J. Bae and H.-J. Yoo, "A 45 μ W injection-locked FSK wake-up receiver for crystal-less wireless body-area-network," in *IEEE Asian Solid State Circuits Conf.*, 2012, pp. 333–336.
- [18] T. Abe, T. Morie, K. Satou, D. Nomasaki, S. Nakamura, Y. Horiuchi, and K. Imamura, "An ultra-low-power 2-step wake-up receiver for IEEE 802.15.4g wireless sensor networks," in *Symp. on VLSI Circuits Dig. of Tech. Papers*, 2014, pp. 1–2.
- [19] C. Salazar, A. Kaiser, A. Cathelin, and J. Rabaey, "A -97dBm sensitivity interferer-resilient 2.4GHz wake-up receiver using dual-IF multi-n-path architecture in 65nm CMOS," in *IEEE Int. Solid-State Circuits Conf.*, 2015, pp. 1–3.
- [20] C. Bryant and H. Sjöland, "A 2.45GHz, 50 μ W wake-up receiver front-end with -88dBm sensitivity and 250kbps data rate," in *Eur. Solid State Circuits Conf.*, September 2014, pp. 235–238.
- [21] X. Huang, P. Harpe, G. Dolmans, H. de Groot, and J. R. Long, "A 780–950MHz, 64–146 μ W power-scalable synchronized-switching OOK receiver for wireless event-driven applications," *IEEE J. of Solid-State Circuits*, 2014.
- [22] H. Milosiu, F. Oehler, M. Eppel, D. Fruhsorger, S. Lensing, G. Popken, and T. Thones, "A 3 μ W 868MHz wake-up receiver with -83dBm sensitivity and scalable data rate," in *Proc. of the Eur. Solid State Circuits Conf.*, 2013, pp. 387–390.
- [23] T. Copani, S. Min, S. Shashidharan, S. Chakraborty, M. Stevens, S. Kiaei, and B. Bakkaloglu, "A CMOS low-power transceiver with reconfigurable antenna interface for medical implant applications," *IEEE Trans. on Microwave Theory and Techn.*, vol. 59, no. 5, pp. 1369–1378, 2011.
- [24] S. J. Marinkovic and E. M. Popovici, "Nano-power wireless wake-up receiver with serial peripheral interface," *IEEE J. on Select. Areas in Commun.*, vol. 29, no. 8, pp. 1641–1647, 2011.
- [25] S. Drago, D. Leenaerts, F. Sebastiano, L. J. Breems, K. A. Makinwa, and B. Nauta, "A 2.4GHz 830pJ/bit duty-cycled wake-up receiver with -82dBm sensitivity for crystal-less wireless sensor nodes," in *IEEE Int. Solid-State Circuits Conf. Dig. Tech. Papers*, 2010, pp. 224–225.
- [26] P. Le-Huy and S. Roy, "Low-power wake-up radio for wireless sensor networks," *Mobile Networks and Appl.*, vol. 15, no. 2, pp. 226–236, 2010.
- [27] C. Hambeck, S. Mähknecht, and T. Herndl, "A 2.4 μ W wake-up receiver for wireless sensor nodes with -71dBm sensitivity," in *IEEE Proc. Int. Symp. Circuits and Syst.*, 2011, pp. 534–537.
- [28] Y. Wei, J. Heidemann, and D. Estrin, "An energy-efficient MAC protocol for wireless sensor networks," in *Proc. 21st Ann. Joint Conf. IEEE Comput. and Commun. Soc.*, vol. 3, 2002, pp. 1567–1576.
- [29] H. Sjöland *et al.*, "Ultra low power transceivers for wireless sensors and body area networks," in *8th Int. Symp. Medical Inform. and Commun. Technology*, April 2014, pp. 1–5.
- [30] N. S. Mazloum and O. Edfors, "Performance analysis and energy optimization of wake-up receiver schemes for low-power applications," *IEEE Trans. Wireless Commun.*, vol. 13, pp. 7050–7061, 2014.
- [31] H. Sjöland *et al.*, "A receiver architecture for devices in wireless body area networks," *IEEE J. Emerg. Sel. Topic Circuits Syst.*, vol. 2, pp. 82–95, March 2012.
- [32] S. Y. Seidel and T. S. Rappaport, "914 MHz path loss prediction models for indoor wireless communications in multifloored buildings," *IEEE Trans. on Antennas and Propagation*, vol. 40, no. 2, pp. 207–217, 1992.
- [33] M. Lont *et al.*, "Analytical models for the wake-up receiver power budget for wireless sensor networks," in *Proc. 28th IEEE Global Telecommun. Conf.*, 2009, pp. 1146–1151.
- [34] N. S. Mazloum, J. N. Rodrigues, O. Andersson, A. Nejdel, and O. Edfors, "Improving practical sensitivity of energy optimized wake-up receivers: proof of concept in 65nm CMOS," *Under review for publication in IEEE Sensors Journal. (Manuscript available on arXiv.org arXiv:1605.00113)*, 2016.